Investigation of Coordination Geometry Around Iron in Annealed Sapphire (Al_2O_3) Using PL, XRD, XAS and FTIR Techniques

K. S. Jheeta* and D. C. Jain
Department of Physics, University of Rajasthan, Jaipur 302004, India

X-ray absorption (XANES and EXAFS) measurements have been performed at room temperature to characterize the valence state and environment around Fe atom in pristine and sapphire heated to 1000°C. Signature of increased valence state is observed in heated sapphire in addition to distortion of octahedral symmetry. Reduction in Fe-O distance in heated sapphire reflects a change in the crystal field around Fe atom. Results are interpreted in terms of Fe(3d) O(2p) hybridization. Photoluminescence spectrum indicates a reduction in oxygen vacancy centers upon heating. The role of oxygen vacancies is discussed in terms of change in valence and crystal field around Fe atom. A change in lattice parameters determined by X-ray diffraction in heated sapphire further confirms the reduction in bond length between Fe and O atoms. Fourier transform infrared (FTIR) spectroscopy is undertaken to see changes in bonding between Al and O atoms or structural changes in the sapphire on heating.

1. Introduction

Aluminium oxide (Al_2O_3), commonly called sapphire, is one of the ceramic materials, which serves as a standard for many high temperature studies [1-3]. Al_2O_3 doped with transition metal ions (Fe, Ti etc) is known to be an important ceramic and laser crystal material [4-7]. Nonstoichiometry, defects and impurities such as transitional metal ions are typical contaminants in growth process in wide gap material such as Al_2O_3. Amongst impurities encountered in Al_2O_3, Ti, Fe, and Cr are known to have important effects on its mechanical, optical and electrical properties [8]. Proper application of this material, especially in the hostile environment of high temperature and radiation, requires an understanding of the effect of its coordination geometry and bonding due to the presence of defects and impurities. Moreover, defects and impurities have a great influence in the high temperature properties such as plastic deformation and creep resistance [9]. This is because mass transport properties of Al_2O_3 are altered as a result of a change in the point defect environment [10]. The optical properties (i.e., color) of Al_2O_3 depend on the impurities ions. For instance, Al_2O_3 becomes red when Cr^{3+} ions substitutes for Al^{3+} ions. Similarly Al_2O_3 becomes yellow with Fe substitution. In another case, Al_2O_3 becomes blue in the presence of both Fe^{2+} and Ti^{4+}. An obvious implication is that impurities play an important role in the macroscopic properties of this material [11, 12].

* Corresponding author: kuldeep_jheeta@yahoo.com

Therefore, the determination of the local structure around impurity is essential as a first step to understand the specific macroscopic properties of these materials.

The crystal structure of Al_2O_3 belongs to the space group R_3c. The rhombohedral unit cell contains two Al_2O_3 formulas. Aluminium ions are linked to six oxygen ions in distorted octahedron. The six oxygen atoms are gathered into two groups of three atoms each. These groups lie at two different distances from the central atom. The farther three oxygen atoms compose the face shared by two joined octahedral, while nearest three oxygen atoms are an edge shared by two joined octahedral. The ionic radii of the paramagnetic impurity are larger than the ionic radii of aluminium atoms (r_{Fe}^{3+} = 0.645 A and r_{Al}^{3+} = 0.615 A in an octahedral site). This imposes a strong relaxation in the material [13].

Therefore, natural sapphire containing oxygen vacancies has been subjected to heat treatment to investigate variation in the concentration of oxygen vacancies and its effect on the valence state of trace element, bond lengths (M-O or M-Al distances, M stands for trace element), symmetry, and crystal field around trace element. We have selected Fe as one of the trace element for investigation under XANES and EXAFS techniques to provide this information. X ray spectroscopy is a well-established technique and a powerful tool for the characterization of materials highly sensitive to arrangement of atoms around the absorbing atom, a fact that reflects the existence of unoccupied electronic states in the absorbing atom. This technique is being employed frequently for the

study of complex systems and with increasing degree of success even for minerals [14, 15]. It was worthwhile therefore to apply it to pristine (unheated) and heated sapphire with a view to investigate the changes in the valence states of Fe ion, coordination symmetry and distortion in structure that take place in atomic environment around the Fe atom on heating. The position and the shape of the pre–peak, the absorption edge, the principal absorption maximum (PAM), and various other features in the XANES region give reliable information about the valence state of absorbing ion and the symmetry of surrounding near-neighbors [14, 15]. XANES is essentially sensitive to the local atomic environment around the absorbing atom. The shape of the XANES spectra depends essentially on the coordination geometry around the metal ions. The extended x-ray absorption fine structure (EXAFS) region of a XAS provides the quantitative information about the coordination number, inter-atomic distance and oxidation state of the impurity ion.

In addition to XANES and EXAFS techniques, photoluminescence (PL) measurements are done to see the changes in oxygen vacancy concentration, X-ray diffraction (XRD) for changes in lattice parameters and Fourier transform infrared (FTIR) for changes in bonding (or structural changes) between Al and O atoms in the sapphire on heating.

2. Experimental Procedure

The South African natural sapphire is used in this study. Samples are prepared by cutting a piece of sapphire to 5x5x1 mm^3 size and cleaned using ethanol in ultrasonic vibrator before heating. These samples consist of 1500 wt. ppm of Fe, 750 wt. ppm of Ti and Cr in traces. The heating is carried out in a furnace in presence of air for 19 hours and at 1000 ^oC. It is done gradually by raising the temperature at a rate of 3 ^oC per minute and also cooled gradually at the same rate. Two unheated samples are kept as pristine. The pristine and heated samples are characterized using the photo-luminescence, the X-ray diffraction, the X-ray absorption, and the Fourier transform infra red spectroscopic techniques. The photoluminescence measurements are carried out at room temperature for two samples of pristine and heated sapphire. These measurements are carried out using Mechelle-900 spectrograph, using 442 nm, He-Cd laser excitation at Inter-University Accelerator Centre (IUAC), New Delhi, India. X-ray diffraction measurements are performed at room temperature at IUAC, New Delhi, using Cu Kα (λ= 1.5406 A) radiation. In order to limit the lateral divergence of the beam, a slit of 0.05 mm was introduced in the incident path of rays before the sample.

All XAFS measurements have been done at room temperature on the face parallel to the plane (0001). XAFS measurements at the Fe edge have been performed at beam line BM 32, ESRF, France, with a photon flux of the order of 10^{11} photons/s. We have made a large number of scans, where in each scan taking a step of ~ 0.4 eV at the beam current ~ 90-100 mA. We measured spectra in fluorescence yield mode of detection with Si diode pairs oriented towards the sample. The recorded spectra are first normalized to the incident photon intensity and then corrected for pre- and post-edge background. Fe-K edge XANES spectra of the heated sapphire and pristine sapphire were normalized with respect to the corresponding edge jumps after a removal from the background. The final pre-edge absorption structure is obtained by subtracting the interpolated arctangent fit to the main edge region of the XANES spectrum. Fe-K absorption edge is determined using the first derivative of XANES spectra, while the fine structure features, including the pre-absorption edge, are determined using a second derivative of XANES spectra.

In our EXAFS analysis, background reduction, Fourier transforms into k- and R-space and the non-linear least squares fit are all done using the UWXAFS packages. A cluster of 81 atoms with Fe as the central absorbing atom is generated using the ATOMS 2.36, which generates the input files to be required by FEFF 800 code to calculate differential computational XAFS paths. Potentials, phase shifts, amplitudes, and the various scattering paths that contribute to the theoretical EXAFS are then generated by running the FEFF 800 program using cluster of 81 atoms. Computational amplitudes envelope and phase shift function of a Fe-O pairs are calculated using FEFF 800 code that also generate the required XAFS paths. Presuming that Fe replaces only the Al cations site atoms in the system, we replaced only one Fe atom with Al atom for fitting purposes. Then, we have subtracted the pre and post-edge atomic absorption backgrounds using the AUTOBK program that provides for subtraction of an energy-dependent atomic absorption. The EXAFS signals are fitted by non-linear least squares fitting using FEFFIT 2.54 program. The number of independent parameters in the present analysis is $N_{ind} \sim (2\Delta k\, \Delta R)/\pi$, for the fit, where Δk and ΔR are the ranges in k and R spaces, respectively.

The infra red spectra for pristine and heated samples of sapphire are recorded in the range 400-4000 cm^{-1} using Pye-Unicam SP3-300 spectro-photometer at IUAC, New Delhi.

3. Results and discussions

3.1 Photoluminescence study

The photoluminescence spectra for pristine and heated sapphire are depicted in Fig.1. The bands observed in the photoluminescence spectra are overlapped with each other due to their finite width. Therefore, curve fitting has been done for both the photoluminescence spectra (shown in Fig. 1a) to measure the position and area corresponding to each band. As can be seen from the Fig. 1a (i), pristine consists of mainly two bands: one centered around 2.52 eV and the other around 2.32 eV, corresponding to F_2 and F_2^{2+} defect centers, respectively. Positions of these bands are reasonably in good agreement with earlier reported values [16-18]. It is clear from the Fig. 1a (ii) that the area under each band is found to decrease in the heated sample. This indicates the decrease in the concentration of oxygen vacancies in the heated sample.

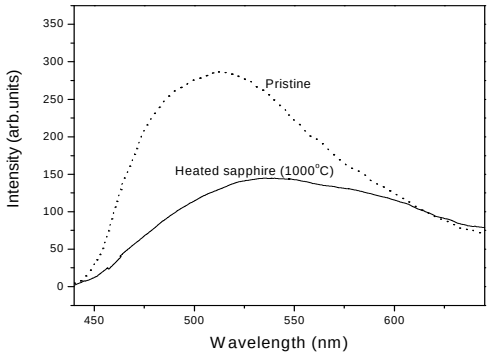

FIG.1: Photoluminescence spectra of pristine and heated sapphire.

The observational data above demonstrate a decrease in oxygen vacancies when samples are heated. Such a decrease may be assigned to annihilation of vacancies due to penetration of oxygen atoms from environment, namely, the oxidation process [19].

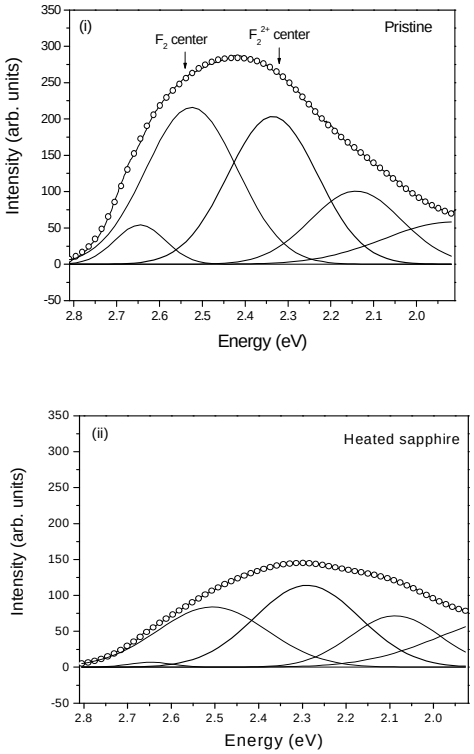

FIG.1a: Gaussian fitted spectra of (i) pristine and (ii) heated sapphire.

3.2 X-ray diffraction study

XRD data of pristine and heated sapphire, at room temperature, are shown in Fig. 2 in 2θ ranges from 25-80°. No change in phase of sapphire is observed after heating. However, the width and positions of basic peaks (104), (110), (113), (204), (116), and (214) are found to change on heating, which leads to change in lattice parameters. The structure parameters are determined by the Rietveld refinement for X-ray patterns. The derived values of lattice constant are 4.7447 and 12.950 Å for pristine and for heated sapphire these values decrease to 4.7412 and 12.936 Å. An increase in intensities in heated sapphire indicates an improvement in crystal structure.

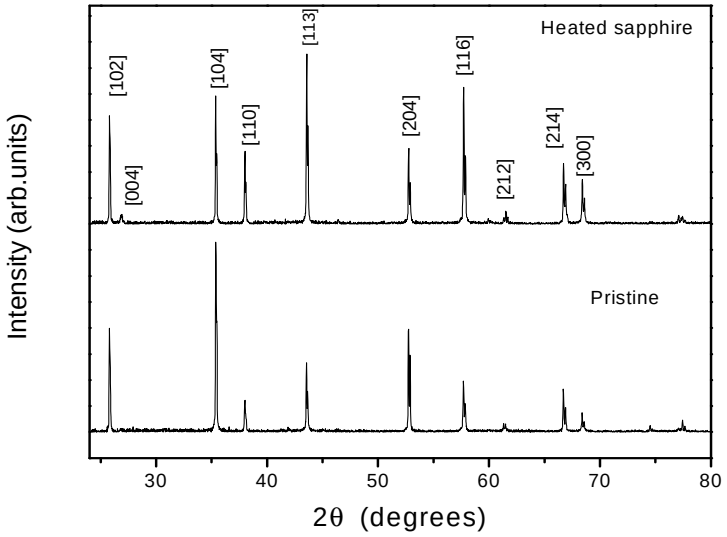

FIG.2: X-ray diffraction spectra of pristine and heated sapphires.

3.3 X-ray absorption study

(i) Fe K-edge XANES

Normalized and background corrected Fe K-edge XANES spectra for pristine and heated sapphire are shown in Fig. 3a. These two spectra look similar qualitatively, but differ slightly in intensities. Both the spectra show a large amplitude near the edge that smoothes out rapidly within 100 eV in both samples.

The energy positions of pre-edge peaks (P_1 & P_2), absorption edge (A), principal absorption maximum (C) and shoulder B before PAM are extracted from first and second derivatives of the absorption spectra.

Pre-edge feature

Pre-edge structure is weak in intensity as shown in Fig. 3a and the subsequent relevant part (after magnification) of the XAS spectrum is shown in Fig. 3b. Pre-edge peaks designated as P_1 and P_2 appear at 7113.6 and 7115.1 eV in pristine. This is in agreement with the reported values of pre-edge peaks for Fe_2O_3 [20, 21]. Pre-edge structure are strong in intensity for tetrahedral coordination, whereas extremely weak or zero for regular octahedral coordination [14, 22]. A distorted octahedral allows a partial mixing of 2p states of oxygen and 3d states of iron. A measurable intensity of these peaks, observed in pristine, suggests the distorted octahedron symmetry around Fe atom in pristine [14, 22]. These peaks correspond to 1s→3d transition and are thus dipole forbidden, but it becomes partially allowed by mixing of the d-states of the transition metal ions with the p-states of the surrounding oxygen atoms [23-25]. It may also be associated with mixing of its own 4p states [26-28]. The 3d state of iron splits into $3d(t_{2g})$ and $3d(e_g)$ levels by crystal field. In this configuration, $3d(e_g)$ state points toward the oxygen legends leading to more hybridization between $3d(e_g)$ and O(2p) states as compared to $3d(t_{2g})$-O(2p) states [29].

The energy position of the pre-edge peaks of pristine sapphire is consistent with Fe ion being mainly in trivalent state [14]. These are commonly related to the presence of several final states arising from the crystal field splitting [14, 28]. However, contribution such as coexistence of the several oxidation states cannot be ruled out [14, 28]. These peaks (P_1 and P_2) may be assigned to $1s \rightarrow 3d(t_{2g})$ and $1s \rightarrow 3d(e_g)$ transitions, respectively. The pre-edge peak corresponding to Fe^{2+} ion appearing at 7112 eV [14, 28] is not observed either due to poor detection limit or low Fe^{2+}/Fe^{3+} ratio. Hence it can be concluded safely that Fe atom in the pristine is in trivalent state and in distorted octahedron symmetry.

The energy position of peak P_1 remains same while a shift of 0.1 eV is observed for peak P_2 in heated sapphire. The area under the peaks are measured by curve fitting analysis and tabulated in Table 1.

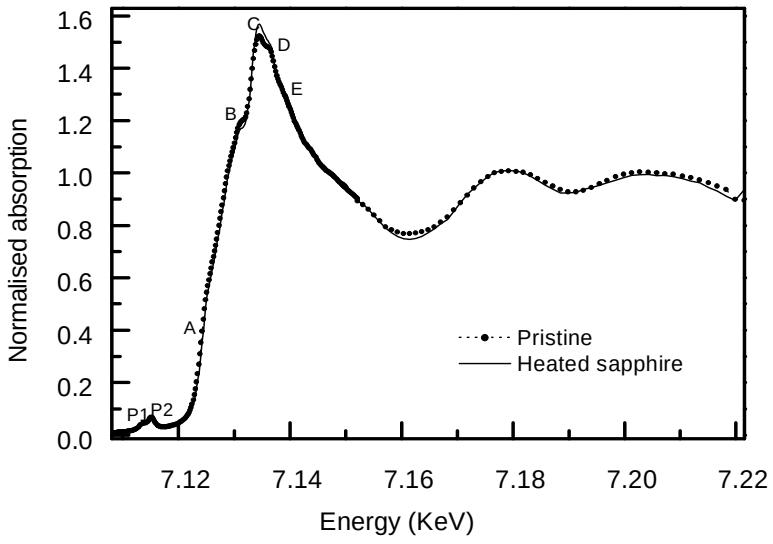

FIG.3a: Fe k-edge XANES spectra of pristine and heated sapphire.

The area under the peak P_2 is comparatively large in heated sample. This could be due to the change in the local environment around Fe ion. Since pre-edge peaks appear as a result of the hybridization of the 2p oxygen orbital with the 3d states of iron, a relatively higher intensity of peak P_2 suggests more intimate mixing of O(2p) states with the 3d(e_g) states of iron. Further, an increase of 0.1 eV in the energy separation observed between the peaks for the heated sample suggests an increase in the crystal field around Fe atom. Therefore, a slight decrease in Fe-O distance is expected.

Main K-absorption edge

The Fe K-absorption edge (A) is observed at 7124.2 eV in pristine (Fig. 3a). Absorption edges are reported around 7121.8 eV and 7124.8 eV in Fe^{2+} and Fe^{3+} compounds, respectively [30]. This suggests us to infer the valence state of iron in sapphire to be trivalent. A shift of 0.3 eV towards high-energy side in heated sapphire may be assigned to an increase of valence state of iron [31, 32].

Feature B, 3.1 eV before the principal absorption maximum, appears at 7130.6 eV. This is assigned to the shakedown process in pristine. The intensity of this feature is reduced slightly (shown in Fig. 3c) and shifted to high-energy side on heating.

The principal absorption maximum (C) is observed at 7133.7 eV in pristine, showing a contribution of 1s → 4p transition. This shifts to higher energy side by 0.4 eV with a slight increase in intensity in heated sapphire can be seen in Fig. 3c. It may be due to change in both the valence and coordination geometry of the Fe atom [33, 34].

(ii) Fe K-edge EXAFS

The local structures around Fe atom in Al_2O_3 have been determined quantitatively by EXAFS. Fig. 4 shows the plots of the x-ray absorption coefficient, $\mu(E) = \log (I_o/I)$, of the pristine and sapphire heated to a temperature of 1000°C after background subtraction and normalization process. The EXAFS spectra in the k space (2.0 to10 $Å^{-1}$) are Fourier transformed to the radial distribution function (RDF) and is shown in Figs. 5a and 5b, respectively.

The FT presented here is not corrected for the phase shift due to photoelectron back scattering and represents only the raw experimental data. A reasonably high signal to noise ratio is evident from the EXAFS spectrum as well as from the Fourier transforms.

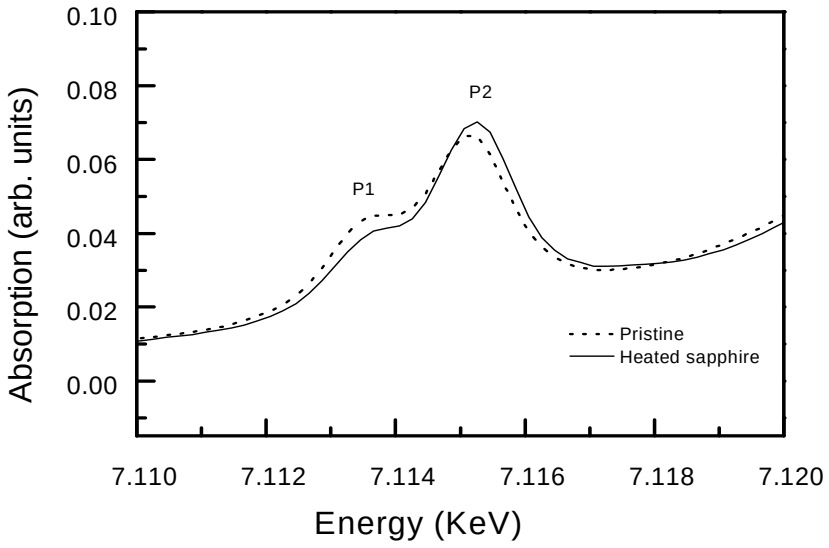

FIG. 3b: Pre-edge peaks of pristine and heated sapphire.

Table 1: Gaussian fitted parameters for pristine and heated sapphire.

Sample	P_1				P_2			
	Pos. (eV)	Area	FWHM	Height	Pos. (eV)	Area	FWHM	Height
Pristine	7113.6	3.01×10^{-5}	0.0012	0.019	7115.1	5.18×10^{-5}	0.0011	0.037
Heated	7113.6	2.26×10^{-5}	0.0012	0.015	7115.2	5.87×10^{-5}	0.0011	0.040

From Fig. 5a, one can observe that three Fourier transform (FT) peaks of large magnitude appear within the unit cell size and other small FT peaks beyond it. In general, the FT peaks above one unit cell parameter size are due to the number of single and multiple scatterings. The contribution of single and multiple scattering paths is very difficult to separate because of their overlapping. Therefore, only four scattering paths are considered important for the determination of correct structural information.

The first FT peak in the range 0.9 - 2.0 Å corresponds to six coordinated oxygen atoms around the Fe atom [35], while the second FT peak in the range 2.0 - 2.9 Å can be assigned to contributions by Al atoms [35]. Peaks at higher distances (beyond 3 Å) are well defined, indicating a good crystalline character of both the samples, but comparatively better in the heated one.

The radial distribution function (RDF) curve of pristine and the determined structural parameters (i.e., degeneracy, near neighbours and Debye-Waller factor) are given in Table 2. The first peak correspond to three O_1 at distance 1.96 Å and another three O_2 at distance 2.07 Å from Fe atom, while the second peak that appears at 2.78 Å is due to distance of Al atoms from Fe atom. The metal-oxygen (Al-O) bond lengths are 1.86 and 1.97 Å for α-Al_2O_3 [36], while 1.94 and 2.11 Å for Fe_2O_3 [35, 37]. Here these values are very close to Fe_2O_3. On

the contrary, the Fe-Al distances are in between the Al-Al distance (2.65 Å) in α-Al_2O_3 and Fe-Fe distance (2.90 A) in α-Fe_2O_3. The RDF curve of heated sapphire is shown in Fig. 5b and fitted parameters are also given in Table 2. The bond lengths corresponding to Fe-O_1 and Fe-O_2 are observed at 1.88 and 1.99 Å, respectively.

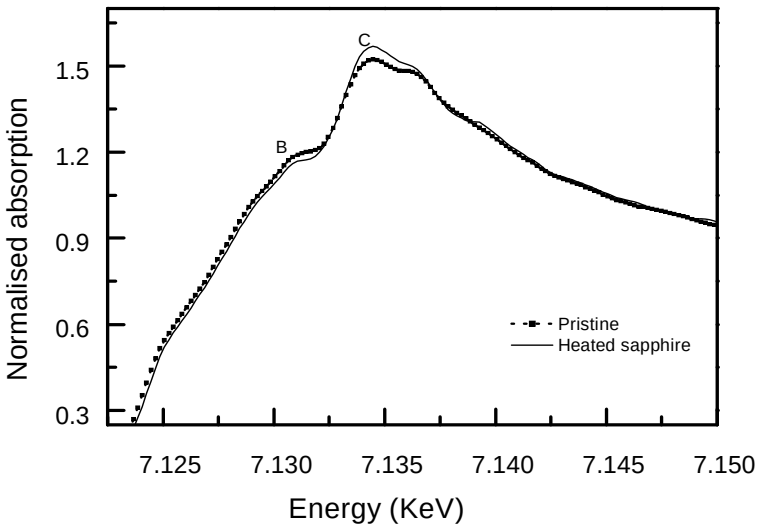

FIG.3c: Principal absorption maximum (PAM) of pristine and heated sapphire.

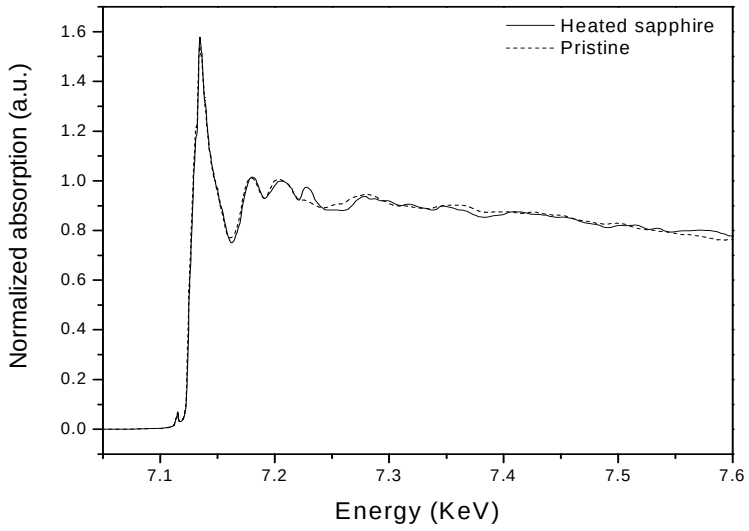

FIG.4: X-ray absorption spectra of pristine and heated sapphire.

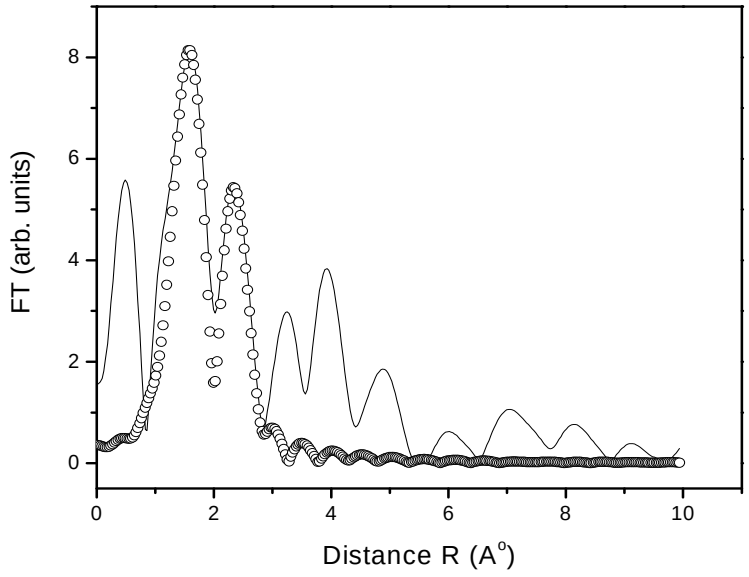

FIG.5a: The Fourier transform of EXAFS' oscillations of pristine sapphire. Spectra with solid curves represent the experimental data and curve made of circles represents the fitted data.

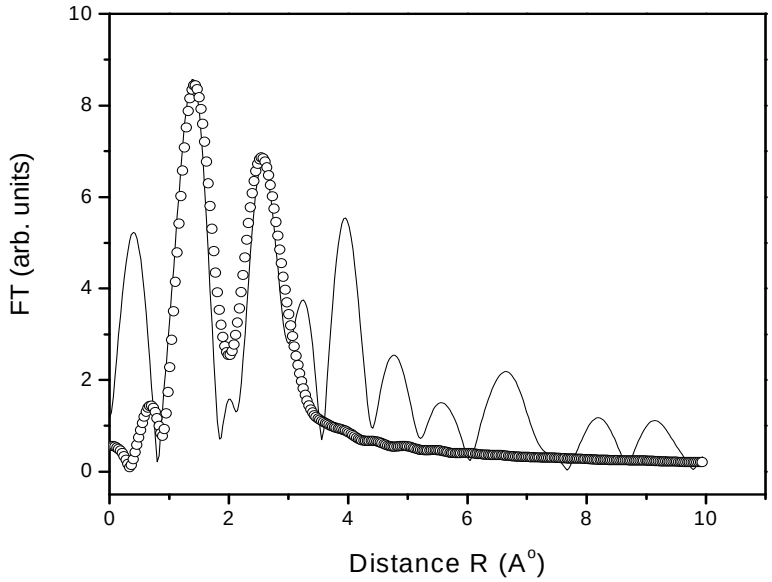

FIG.5b: Fourier transform of the EXAFS oscillations of heated sapphire. Spectral curve (solid) represents the experimental data and those with circle "o" represents the fitted data.

Table 2: Structural parameters from EXAFS spectra analysis for pristine and heated sapphire.

Sample		Path	N (atoms)	R (Å)	Δr	σ^2 (Å^2)	r-factor
Pristine	1st peak	Fe-O_1	3.0	1.95	0.093	0.00755	0.04
		Fe-O_2	3.0	2.07	0.098		
	2nd peak	Fe-Al_1	1.0	2.78	0.13		
Heated sapphire	1st peak	Fe-O_1	3.0	1.88	0.015	0.00389	0.08
		Fe-O_2	3.0	1.99	0.016		
	2nd peak	Fe-Al_1	1.0	2.67	0.022		
		Fe-Al_2	3.0	2.83	0.022		

The decrease in the (Fe- O) bond length can be seen and it is in agreement with our earlier conclusion regarding Fe-O distance derived from pre-edge structure studies and seems to approach towards (Al-O) bond distance. It has been reported that (impurity metal–O) distances increases with the concentration of oxygen vacancies created by ion irradiation [38]. Therefore, a decrease in impurity ion-O bond length is a strong evidence of reduction in oxygen vacancies. This is also expected in the case of heated sapphire attributable to oxidation process. It is still an open question as to how Fe-O distance approaches Al-O distance in heated sapphire. This is left for future work. Further, X-ray diffraction analysis also favours a decrease in Fe-O bond length on heating.

The second peak between 2.0 – 2.9 Å^{-1} in FT spectrum is due to near next neighbour (Al). The amplitude is higher in the case of heated sapphire suggesting that a comparatively large number of Al atoms exist around Fe ion in heated sapphire. This implies that the coordination number around Fe atom has increased.

3.4 Fourier Transform infrared spectroscopic measurements

The infrared (IR) spectrum of pristine and sapphire heated at 1000^o C is shown in Fig. 6. The pristine spectrum shows bands peaked at 487, 518, 628, and 760 cm^{-1}. The bands at 760 and 628 cm^{-1} are attributed to Al-O-Al stretches of the octahedral molecules (asymmetric ν_{as} and symmetric ν_s stretches of the bride bonds, respectively). The band at 487 cm^{-1} is due to the deformation mode ν_d of those bands [39]. These bands are observed at 487, 519, 628, and 761 cm^{-1} in heated sapphires. It is observed that the intensity of the bands increases and some of them are shifted to higher wave number. The higher intensity of ν_{as}, ν_s and ν_d bands suggests that bonding between Al and O is strengthened upon heating and the observed shift of these bands may be correlated with the changes in the Al-O distances. This may be due to the annihilation of oxygen vacancies in the material on heating.

4. Conclusions

The following set of conclusions is the result of above discussion and can be summarized as follows:

1. The energy difference between pre-edge peaks measured from the pre-edge structures of XANES spectra changes from 1.5 eV in unheated sample to 1.6 eV in the heated sample. An increase of 0.1 eV is associated with a change in crystal field splitting around Fe atom leading to more mixing of 3d-2p states and consequently shorter Fe-O distance is observed.
2. The energy positions of pre-edge peaks suggest the trivalent state of Fe ion in pristine and its heated sample, but no signature for Fe^{2+} is seen. Further, weak intensity of these peaks suggests the distorted octahedral symmetry around Fe atom.
3. The increased intensity of PAM along with its shifts towards the higher energy side supports the oxidation phenomenon upon heating.
4. From EXAFS analyses, Fe-O distance in pristine is observed at 1.95 and 2.07 Å. These bond distances reduce to 1.88 and 1.99 Å upon heating. This shows a

structural relaxation around Fe atom that could be due to the annihilation of oxygen vacancies in the lattice.

5. The changes in the position and intensity of the second shell (Fe-Al) reflect a change in local symmetry around the Fe atom.
6. From photoluminescence spectra, it is clear that pristine sample contains a certain amount of oxygen vacancies, which decreases upon heating.
7. Fourier transform infrared measurements show that the bonding between Al and O atoms is strengthened upon heating. A shift in some of the IR bands towards high wave number indicates the change in the Al-O distance.

In conclusion, oxygen vacancies play an important role in deciding the symmetry around the absorbing atom and the information (pre-edge and main edge) derived from XANES can be used as a sensitive indicator of a change in local environment or distortion around the central atom.

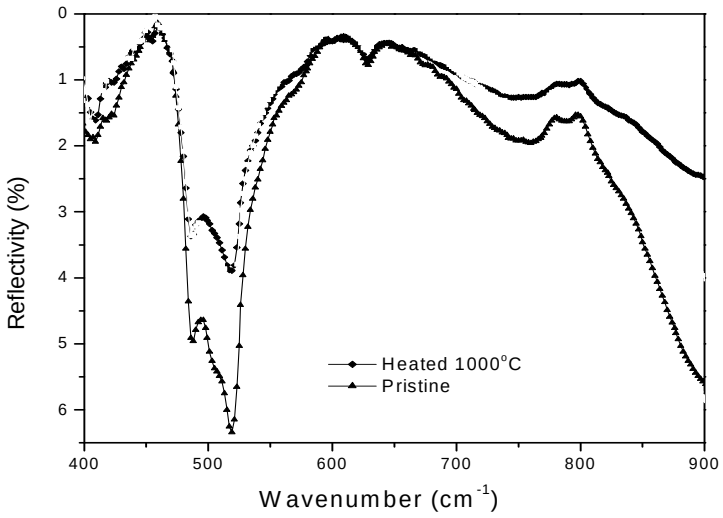

FIG.6: IR reflection spectra of pristine and heated sapphires.

Acknowledgments

One of the authors, (KSJ) is highly grateful to the Director and the Associates Office of the Abdus Salam International Centre for Theoretical Physics (ICTP), Trieste, Italy, for utilizing its library facility to collect scientific material. We are thankful to the ESRF, France, to carry out X-ray absorption measurements and Inter University Accelerator Center (IUAC), New Delhi to carry out X-ray diffraction, photoluminescence and IR measurements.

References

[1] P. Aldebert and J. P. Traverse, High Temp. - High Pressure **16**, 127 (1984).

[2] J. B. Wachtman Jr., T. G. Scuderi and G.W. Cleek, J.Am. Cerem. Soc. **45,** 319 (1962).

[3] R. G. Munro, J. Am. Cerem. Soc. **80**, 1919 (1997).

[4] W. L. Yu and J. L. Wang, Phys. Stat. Solidi (b) **176**, 433 (1993).

[5] W. C. Zheng, Physica **B245**, 119 (1998).

[6] J. Y. Buzare, G. Silly, J. Klein, G. Scholz, R. Stosser and M. Nofz, J. Phys. Cond. Matter **14**, 10331 (2002).

[7] W. Lu, X-Y Kuang, K-W Zhou and D. Die, J. Phys. Chem. Solids **65**, 1147 (2004).

[8] K. Nassau, "Gems made by Man", (1980).

[9] H. Yoshida, Y. Ikuhara and T. Sakuma, J. Mater. Res. **13**, 249 (1998).

[10] A. H. Heuer and K. P. D. Lagerlof, Philos. Mag. Lett. **79**, 619 (1999).

[11] K. Nassau, *The Physics and Chemistry of color* (Wiley Interscience, 1983).

[12] S. Lee, C. M. Bradbeck and C. C. Yang, Phys. Rev. **B15**, 2469 (1997).

[13] R. D. Shannon, Acta. Cryst. **A32**, 751 (1976).

[14] M. Wilke, F. Farges, P. E. Petit, G. E. Brown Jr. and F. Martin, Am. Miner. **86**, 714 (2001).
[15] P. A. Van Aken, B. Liebscher and V. J. Styrsa, Phys. Chem. Miner. **25**, 323 (1998).
[16] X. Wang, J. Lei, D. Wang and N. Huang, J. Mater. Sci. Technol. **21**, 871 (2005).
[17] B. D. Evans, G. J. Pogatshnik and Y. Chen, Nucl. Instr. and Meth. **B91**, 258 (1994).
[18] K. S. Jheeta, D. C. Jain, Fouran Singh, Ravi Kumar and K. B. Garg, J. Nucl. Mater. **353**, 190 (2006).
[19] P. Winotia, T. Wichen, I. M. Tang and J. Yaokulbodee, Int. J. Mod. Phys. **B14**, 1693 (2000).
[20] G. Drager, R. Frahm, G. Materlik and O. Brummer, Phys. Stat. Solid **B146**, 287 (1988).
[21] W. A. Caliebe, C. C. Kao, J. B. Hastings, M. Taguchi, A. Kotani, T. Uozumi and F. M. F. de Groot, Phys. Rev. **B58**, 13452 (1998).
[22] M. G. Kin, H. S. Cho and C. H. Yo, J. Phys. Chem. Solids **59**, 1369 (1998).
[23] G. Giuli, G. Pratesi, C. Cipriani and E. Paris, Geochimica et Cosmochimica Acta **66**, 4347 (2002).
[24] Y. Ma et. al. Phys. Rev. **B48**, 2109 (1993).
[25] J. Zhang, Z. Y. Wu, K. Ibrahim, M. I. Abbas and X. Ju, Nucl. Instr. and Meth. **B199**, 291 (2003).
[26] T. A. Westre, P. Kennepohl, J. de Witt, B. Hedman, K. O. Hodgson and E. I. Solomon, J. Am. Chem. Soc. **119**, 6297 (1997).
[27] D. Heumann, G. Drager and S. Bocharov, J. Phys. IV France **7**, 481 (1997).
[28] F. Farge, Phys. Chem. Miner. **28**, 619 (2001).
[29] L. Senzi, D. George, M. Genge and I. Enrique, J. Phy. Chem. **B105**, 5743 (2001).
[30] S. Kin, T. Ohta and G. Kwag, Bull. Korean Chem. Soc. **21**, 588 (2000).
[31] S. R. Sutton, S. Bajt, J. Delaney, D. Schulze and T. Tokunaga, Rev. Scien. Instr. **66**, 1464 (1995).
[32] A. J. Berry, H. C. O'Neill, K. D. Jayasuriya, S. J. Campbell and G. J. Foran, Am. Miner. **88**, 967 (2003).
[33] S. Bajt, S. R. Sutton and J. S. Delaney, Physica **B208&209**, 243 (1995).
[34] A. C. Scheinost, H. Stanjek, D. G. Schulze, U. Gasser and D. L. Sparks, Am. Miner. **86**, 139 (2001).
[35] E. Gaudry, A. Kiratisin, Ph. Sainctavit, C. Brouder, F. Mauri, A. Ramos, A. Rogalev and J. Goulon, Phys. Rev. **B67**, 094108 (2003).
[36] W. B. Pearson, Structure Reports (International Union of Crystallography, Utretch, 1962), Vol.27.
[37] L. W. Finger and R. M. Hazen, J. Appl. Phys. **51**, 5362 (1980).
[38] D. M. Bhardwaj, D. C. Jain, S. Dalela, Ravi Kumar, N. L. Saini and K. B. Garg, Physica **B350**, 366 (2004).
[39] I. Kh. Abdukadyrova, Inorganic Mater. **41**, 1225 (2005).

Received: 23 August, 2007
Accepted: 9 October, 2007